X-ray Thomson scattering in warm dense matter at low frequencies

Michael S. Murillo*
Physics Division, Los Alamos National Laboratory, Los Alamos, New Mexico 87545, USA
(Received 29 April 2009; revised manuscript received 27 June 2009; published 8 March 2010)

The low-frequency portion of the x-ray Thomson scattering spectrum is determined by electrons that follow the slow ion motion. This ion motion is characterized by the ion-ion dynamic structure factor, which contains a wealth of information about the ions, including structure and collective modes. The frequency-integrated (diffraction) contribution is considered first. An effective dressed-particle description of warm dense matter is derived from the quantum Ornstein-Zernike equations, and this is used to identify a Yukawa model for warm dense matter. The efficacy of this approach is validated by comparing a predicted structure with data from the extreme case of a liquid metal; good agreement is found. A Thomas-Fermi model is then introduced to allow the separation of bound and free states at finite temperatures, and issues with the definition of the ionization state in warm dense matter are discussed. For applications, analytic structure factors are given on either side of the Kirkwood line. Finally, several models are constructed for describing the slow dynamics of warm dense matter. Two classes of models are introduced that both satisfy the basic sum rules. One class of models is the "plasmon-pole"-like class, which yields the dispersion of ion-acoustic waves. Damping is then included via generalized hydrodynamics models that incorporate viscous contributions.

DOI: 10.1103/PhysRevE.81.036403 PACS number(s): 52.27.Gr, 61.05.cf, 52.25.Jm

I. INTRODUCTION

X-ray Thomson scattering (XRTS) is emerging as a powerful tool for both diagnosing and measuring novel properties of dense plasmas [1]. Of particular interest is the warm dense matter (WDM) regime, which can be loosely defined as matter at about solid density with temperatures up to several ($\sim$10) eV. Here, a specific regime of WDM physics is considered that is defined as matter with Coulomb coupling and degeneracy parameters of order unity [2]. The Coulomb coupling parameter is taken to be the electron-electron coupling parameter, defined here as

$$\Gamma_{ee} = \frac{e^2}{a_e \sqrt{T^2 + E_F^2}}, \tag{1}$$

where $a_e = (3/4\pi n_e)^{1/3}$ is the electron-sphere radius in terms of the electron density n_e. The degeneracy parameter is taken to be

$$\Theta = \frac{E_F}{T}, \tag{2}$$

where E_F is the Fermi energy. All other symbols have their usual meanings. In practice, using these definitions, this regime of WDM is matter with $T \sim 10$ eV and densities about half solid, as will be illustrated below. The reason for considering this specific definition is that the two usual expansion parameters, and their inverses, cannot be used as expansion parameters in this regime. Diagnosing matter in this regime is quite difficult, and XRTS could play an important role; more importantly, generating theoretical descriptions of WDM are equally difficult [3], and XRTS may be the only way to elucidate detailed properties.

WDM occurs in very disparate scenarios. Astrophysical objects such as brown dwarfs and giant planets [4] are composed of matter on the cool side of the WDM parameter space considered here. In the laboratory, intense laser-solid interactions [5] and pulsed power experiments [6] readily form WDM conditions. Understanding the physical properties of such matter is also important for inertial confinement fusion modeling and interpretation. In particular, WDM physics is relevant for fast ignition schemes [7].

Here, I focus on the low-frequency portion of the XRTS spectrum. Because this regime probes ion dynamical properties, it is rich in the physics of strong coupling, including the collective properties of viscous hydrodynamics [8]; for modeling purposes, we wish to know the limitations of applying hydrodynamics to strongly coupled systems such as WDM. Moreover, beyond measuring basic quantities, such as temperature, density, and effective ionization level, we wish to use XRTS to measure ionic transport properties.

I begin by providing a definition of warm dense matter that allows us to delineate temperature-density regimes of interest. Then, a review of the XRTS cross section is given, to recall how ion dynamics enters the measured spectrum. The reduction of WDM to an effective dressed-particle description is considered, with special attention given to various approximations associated with such a description. Different models are given for the WDM static structure factor, including useful analytic forms on both sides of the Kirkwood line. A comparison with liquid metal (Al) data is made. The focus then turns to models of the ion-ion dynamic structure factor (ii-DSF). The models fall into two classes: plasmon-pole-type models that are constructed to satisfy various sum rules, which incorporate constraints imposed by strong coupling, and generalized hydrodynamics models that incorporate viscous damping. Because of the importance to intense laser-solid experiments, which may not be in thermal equilibrium [9], all models are formulated as two-temperature models. Finally, I conclude with a discussion of

*murillo@lanl.gov

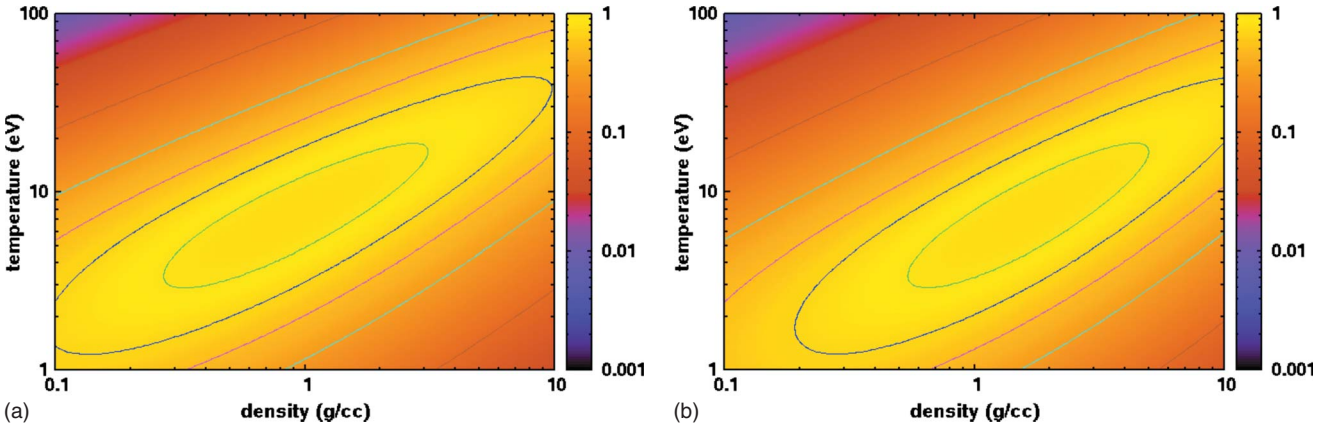

FIG. 1. (Color online) The $\mathcal{W}$ parameter is shown for Be (left panel) and Al (right panel) over wide ranges of temperature and density. The contours are at levels of $\mathcal{W}=0.1,0.3,0.5,0.7,0.9$. Note that the WDM regime captures the center of the phase diagram, away from regions where simplifying assumptions can be made. Also, note that the WDM regime is shifted to slightly higher densities and lower temperatures for higher-Z elements.

several open issues that could form the basis of future research.

II. WARM DENSE MATTER REGIMES

WDM is an ill defined form of matter that can loosely be defined as matter between the traditional hot plasma phase and the cold solid phase. To date, most research has focused on the cool side of this broad regime, including research in astrophysics [10], in nonequilibrium materials science [11], and on warm solids [12], due to the difficulty of generating WDM with higher energy densities. In many cases, the matter produced resembles a liquid metal at elevated temperatures. Here, a portion of the WDM regime that lies above these experiments in temperature is treated. There are several reasons for treating "warmer" WDM. First, future experiments based on much larger drivers, such as those at the National Ignition Facility, will be capable of generating matter throughout an enormous temperature regime. Second, the regime to be considered here is one for which the two most important dimensionless parameters are simultaneously of order unity, making the theoretical treatment considerably more difficult; this difficulty is an important issue for constructing wide ranging equations of state. Third, and related to the second point, the matter treated here has thermal excitation of the atomic core, making the theoretical treatment considerably more difficult than that for WDM at lower temperatures. For all of these reasons, the next few sections are devoted to treating these issues in general, before turning to the main topic of low-frequency XRTS.

WDM is here defined as matter with both $\Theta \sim 1$ and $\Gamma_{ee} \sim 1$. Such WDM is thus matter that is not amenable to purely classical descriptions or ground state quantum descriptions. Furthermore, WDM is not easily treatable by perturbation expansions in the coupling parameter or by disordered lattice models [13]. Most equation of state methods, for example, interpolate through this regime [14]. An important feature of this regime of WDM is partial ionization, due to both temperature and pressure ionization, which is challenging to treat using most theoretical and computational methods; this feature distinguishes WDM from liquid metals, which are treatable by (electronic) ground state methods.

It is important to note that we have taken the coupling parameter to be that of the electron-electron interaction. Not only does this imply nontrivial electron physics, it also implies that the electron-ion and ion-ion interactions are moderate to large. Quantitatively, then, where does this WDM regime lie? Defining a symmetrization function $S(x)=2/(x+x^{-1})$ that peaks when the argument is unity, we can define a "WDM parameter" $\mathcal{W}$ by

$$\mathcal{W}(T,\rho) = S(\Gamma_{ee})S(\Theta), \tag{3}$$

which peaks when $\Gamma_{ee}=\Theta=1$. To relate the variables on either side of the equation, the ionization state is needed, and here a finite-temperature Thomas-Fermi model is used to obtain the connection between (T,ρ) and (Θ,Γ_{ee}). (More will be said about the Thomas-Fermi model in Sec. IV C.) Contour plots of $\mathcal{W}$ are shown in Fig. 1 for Be and Al. This regime of WDM tends to occur at slightly expanded densities, relative to those of a normal solid, and tends to occur at temperatures between a few and several tens of electron volts. The ionization states of Be and Al are shown in Fig. 2. Comparing with Fig. 1, we see that indeed this WDM regime corresponds to the regime where ionization, i.e., important, finite-temperature atomic physics, is beginning to be important, again reinforcing the notion that ground-state methods are not applicable to this WDM. In Fig. 3 the ion-ion Coulomb couplings, defined in the usual way as $\Gamma_{ii}=\langle Z\rangle^2 e^2/(a_i T_i)$, are shown versus temperature and density. (Here, $a_i=(3/4\pi n_i)^{1/3}$ is the usual ion-sphere radius.) Because of the state-dependent ionization level $\langle Z\rangle$, the contours of constant coupling differ greatly between different elements. Interestingly, the couplings are not particularly large, which implies that some regimes of WDM may lie below the Kirkwood line, a subject that will be discussed in detail in Sec. IV E.

It is important to remember that the WDM definition given here is not unique. Often, other definitions are used for

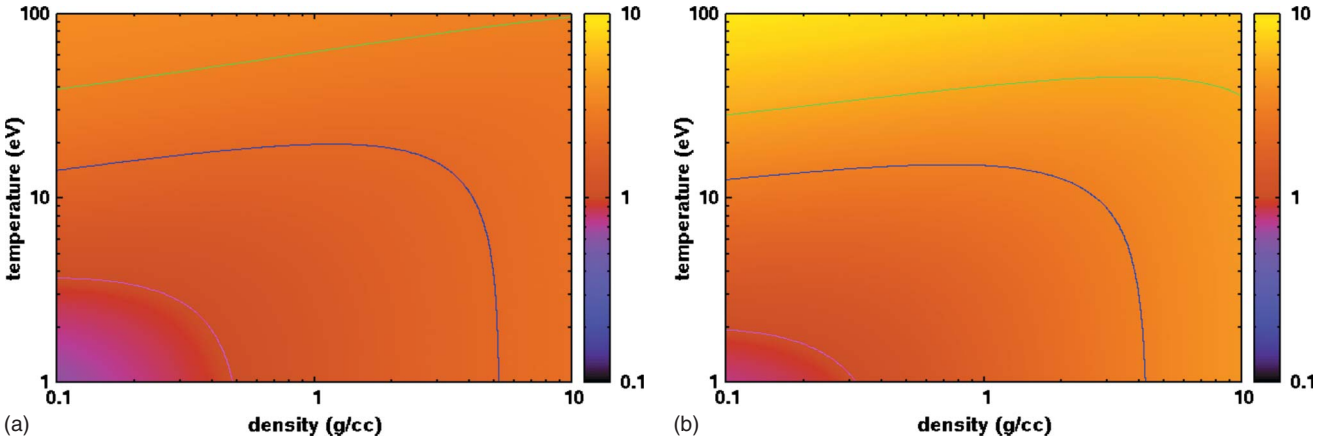

FIG. 2. (Color online) The ionization states of Be (left panel) and Al (right panel) are shown versus temperature and density, as computed with a finite-temperature Thomas-Fermi model. The contours are at ionization states of $\langle Z\rangle = 1.0, 2.0, 3.0$ for Be and $\langle Z\rangle = 1.0, 3.0, 5.0$ for Al. Comparing with Fig. 1, we see that WDM corresponds to matter in which ionization is moderate, thus highlighting the importance of finite-temperature atomic physics. More interestingly, note that WDM occurs along the "knees" of the iso-ionization curves, where temperature and pressure ionization have about equal contributions.

highly excited condensed matter systems [11] that, while still completely degenerate ($\Theta \gg 1$), experience bond breaking that differentiates them from the solid state. Such cooler systems will not be considered here.

III. XRTS CROSS SECTION

The XRTS cross section is usually written as

$$\frac{d^2\sigma}{d\Omega d\omega} = \sigma_T S_{ee}(k,\omega), \tag{4}$$

where σ_T is the Thomson cross section and $S_{ee}(k,\omega)$ is the electron-electron dynamic structure factor (ee-DSF) *for all of the electrons*. Here, $k = 4\pi \sin(\theta/2)/\lambda_0$ is the wave vector in terms of the scattering angle θ and probe wavelength λ_0, and $\omega = (E_0 - E_1)/\hbar$ is the frequency in terms of the scattered photon energy E_1. It is now routine to follow Chihara [15] and write the ee-DSF as the sum of terms

$$S_{ee}(k,\omega) = Z_f S^0_{ee}(k,\omega) + Z_b \int d\omega' S_s(k,\omega') S_{ce}(k,\omega-\omega') + |f(k)+q(k)|^2 S(k,\omega). \tag{5}$$

Here, the first term describes free electron density fluctuations in the presence of a uniform ionic background, and is the term that has received the most attention so far. The second term describes electron-ion coupling contributions that arise from the presence of bound states; note that this term scales as Z_b, the number of bound electrons. The DSFs in this term describe the ion self motion $[S_s(k,\omega)]$ and the response of the core electrons $[S_{ce}(k,\omega)]$. Finally, the third term describes electron density fluctuations driven by the underlying ionic motions, and is therefore proportional to the ion-ion dynamic structure factor $S(k,\omega)$, which is the focus of the present work. The form factors for free and bound electrons that screen the ions are included as $f(k)$ and $q(k)$. Often, the ii-DSF is approximated by its frequency integral

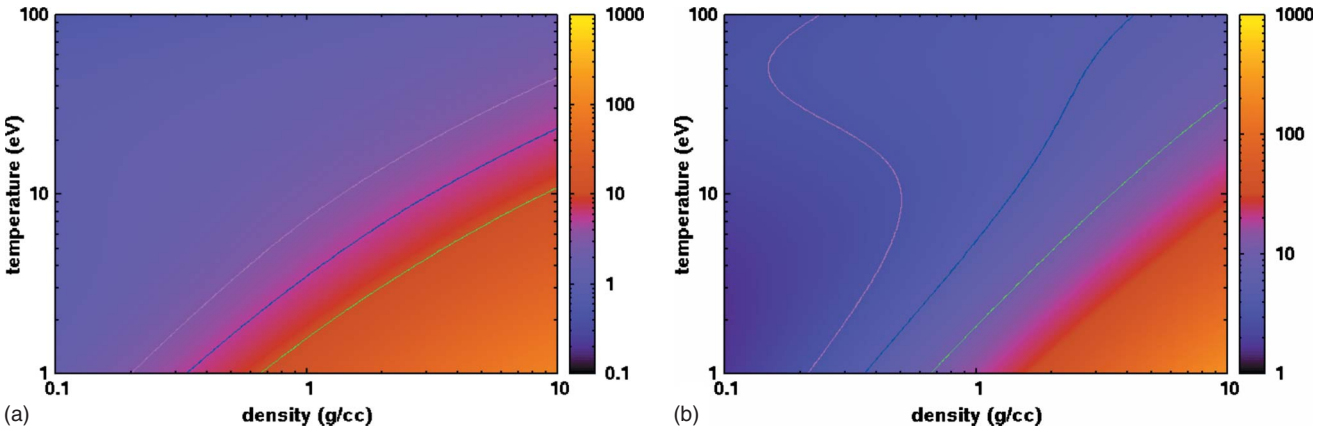

FIG. 3. (Color online) The ion-ion Coulomb coupling parameters for Be (left panel) and Al (right panel). The contours are at levels $\Gamma = 3.0, 5.0, 10.0$. Note that the level of ionic coupling varies from element to element in the WDM regime; here, in the centers of their respective WDM regimes, Al ions are more strongly coupled than Be ions.

[16,17], the static structure factor $S(k)$, which contains far less information. This case will be considered first, in Sec. IV, before turning to dynamics in Sec. V.

IV. DIFFRACTION ONLY

Because of the relatively large ion mass, the simplest form for the ii-DSF can be written as

$$S^{(0)}(k,\omega) = 2\pi \mathcal{A}^{(0)}(k)\delta(\omega), \tag{6}$$

where the coefficient $\mathcal{A}^{(0)}(k)$ is generally unknown, with the superscript 0 denoting the simplest possible model. Typically, $\mathcal{A}^{(0)}(k)$ is determined by the sum rule

$$S(k) = \int_{-\infty}^{\infty} \frac{d\omega}{2\pi} S(k,\omega), \tag{7}$$

which introduces the static structure factor, viz.

$$S^{(0)}(k,\omega) = 2\pi S(k)\delta(\omega). \tag{8}$$

Using such a sum rule approach, the form (8) is unique, because all other sum rules applied to Eq. (6) vanish identically because they involve finite-frequency moments. In this model, the only unknown is the structure factor, and it corresponds to an energy-unresolved measurement (diffraction). Fitting a measurement of $S(k)$ to an accurate model can reveal properties of the WDM, or, if the data are well constrained, can challenge our theoretical models.

A. Reduction to dressed particles

Computing the ion-ion structure factor $S(k)$ in WDM can be greatly facilitated if we can replace the electron-nucleus fluid with an effective, classical system amenable to either integral equation methods, classical Monte Carlo, or classical molecular dynamics. Here, an effective dressed-particle description for WDM is derived both because of the utility of a reduced model and to uncover potentially questionable approximations that may limit the applicability of such an approach to WDM.

WDM is a fluid composed of nuclei and electrons, which are, respectively, classical and quantal. For such a system, the quantum Ornstein-Zernike equations (QOZE) are given by

$$\begin{aligned} h_{NN}(k) &= c_{NN}(k) + n_N c_{NN}(k) h_{NN}(k) + n_e c_{Ne}(k) h_{eN}(k), \\ h_{eN}(k) &= -\frac{\chi_{ee}^{(0)}(k)}{\beta n_e}[c_{Ne}(k) + n_N c_{eN}(k) h_{NN}(k) + n_e c_{ee}(k) h_{eN}(k)], \\ \chi_{ee}(k) &= \chi_{ee}^{(0)}(k)[1 - \beta^{-1} c_{ee}(k)\chi_{ee}(k) + n_N n_e h_{Ne}(k) c_{Ne}(k)], \end{aligned} \tag{9}$$

where N and e denote the nuclei and the electrons, respectively, and $\beta = 1/T$ is the inverse temperature. Details of the QOZE are given in Appendix A. The exact density-density response function for the electrons is given by $\chi_{ee}(k)$, and the Lindhard response is given by $\chi_{ee}^{(0)}(k)$. A useful result, using $S_{NN}(k) \equiv 1 + n_N h_{NN}(k)$,

$$\begin{aligned} \frac{h_{eN}(k)}{S_{NN}(k)} &= -\frac{c_{eN}(k)}{\beta n_e} \frac{\chi_{ee}^{(0)}(k)}{1 + \beta^{-1} c_{ee}(k)\chi_{ee}^{(0)}(k)} \\ &\approx -\frac{c_{eN}(k)}{\beta n_e} \tilde{\chi}_{ee}(k), \end{aligned} \tag{10}$$

results from rearranging the second equation. In the second line, the homogeneous electron gas response function $\tilde{\chi}_{ee}(k)$ has been defined; this is not an exact relation because $c_{ee}(k)$ is the electron-electron direct correlation function in the presence of the ions, whereas the ionic contribution is assumed to be negligible in the second line of Eq. (10). In general, given a suitable quantal closure relation, these equations are quite difficult to solve; the most difficult aspect is obtaining the electronic structure of bound and free states [18].

If the WDM system can be reduced to a dressed-particle system, then we can write

$$g(r) = \exp[-\beta u(r) + h(r) - c(r) + B(r)] \tag{11}$$

for the ions. Since the ions are in the same locations as the nuclei, we have $g(r) = g_{NN}(r)$; the closure relation for the nuclei is

$$g_{NN}(r) = \exp[-\beta u_{NN}(r) + h_{NN}(r) - c_{NN}(r) + B_{NN}(r)]. \tag{12}$$

Using the QOZE [Eq. (9)], these expressions yield the relation (now in Fourier space)

$$u(k) = u_{NN}(k) - \beta^{-1}(B_{NN}(k) - B(k)) - n_e \beta^{-1} \frac{h_{Ne}(k) c_{Ne}(k)}{S_{NN}(k)} \tag{13}$$

between the physics of the electron-nuclei fluid and the dressed interaction. The bridge functions are expected to be small in WDM and will subsequently be dropped. So far, the manipulations have been purely formal and no approximations have been made; without performing an electronic structure calculation [18], it is difficult to proceed.

In order to make progress, we now make the transition from the physical picture to the chemical picture by taking the nuclear variables to be ionic variables that gather together the nuclei and their bound states. The separation of bound and free electrons will be discussed in more detail below. In addition to this approximation, we assume that WDM behaves in a manner similar to liquid metals in that the effective interaction between free electrons and composite ions is weak [19]. The three approximations (including dropping the bridge functions) allow us to write Eq. (13) as

$$u(k) = u_{ii}(k) - n_e \beta^{-1} \frac{h_{ie}(k) c_{ie}(k)}{S_{ii}(k)}. \tag{14}$$

We are now in a position to use the result (10), as extended to the chemical picture, to obtain

$$u(k) = u_{ii}(k) + \beta^{-2}\tilde{\chi}_{ee}(k)c_{ie}^2(k)$$
$$\approx u_{ii}(k) + \tilde{\chi}_{ee}(k)u_{ie}^2(k)$$
$$\approx u_{ii}(k)[1 + u_{ee}(k)\tilde{\chi}_{ee}(k)]$$
$$\approx \frac{u_{ii}(k)}{\tilde{\epsilon}_{ee}(k)}. \quad (15)$$

In the first step, the direct correlation function is expressed in terms of the potential, which is consistent with the assumption of weak electron-ion coupling [19]. In the second step, it is assumed that the interactions are mainly of the Coulomb form, such that $u_{ei}^2(k) \approx u_{ee}(k)u_{ii}(k)$; this is not strictly consistent with the assumption that $u_{ei}(k)$ is weak and should be represented by a pseudopotential, an issue that will be discussed in more detail in Sec. IV B. Finally, the response function is cast in terms of the dielectric function $\epsilon_{ee}(k)$, revealing that these approximations are consistent with a screened ion-ion potential.

Before proceeding, it is worth itemizing all of the approximations that were required in order to obtain Eq. (15). The first and perhaps the most drastic approximation is that we moved from the physical picture to the chemical picture, which avoids a detailed numerical procedure [18]. Next, based on results known from liquid metal conditions [19], the assumption of a weak electron-ion interaction was made, which allowed us make the replacement $c_{ei}(k) \rightarrow u_{ei}(k)$. Note that the remaining direct correlation functions assume their exact forms, with the exception that $c_{ee}(k)$ is taken to be that of the homogenous electron gas in $\tilde{\chi}_{ee}(k)$. Finally, it was assumed that the interactions were roughly of the Coulomb form, which allowed the introduction of the dielectric function. All of these approximations are expected to be reasonable, but little is known about the quantitative errors that have been incurred. With this caveat, in what follows, it will be assumed that the ionic portion of WDM can be replaced with a suitable screened interaction.

B. WDM as a Yukawa system

Computing the structure factor $S(k)$ is a straightforward matter using standard integral equation methods. The simplest method is to assume that the ion-ion interaction potential $u(r)$ is known, and solve for the radial distribution function using the exact equations

$$g(r) = \exp[-\beta u(r) + h(r) - c(r) + B(r)],$$

$$h(r) = g(r) - 1,$$

$$h(k) = \frac{c(k)}{1 - nc(k)}. \quad (16)$$

In addition to knowledge of the interaction potential, one must also specify the bridge function; neglecting this contribution, which is the hypernetted chain approximation, will still yield reasonable results for most WDM systems.

Alternatively, we can choose to model the WDM ion-ion interaction potential in terms of a form for which $B(r)$ is known. Here, we will assume that the ion-ion interaction is of the Yukawa form, which is reasonable for screened Coulomb systems, and for which a very accurate bridge function has been fit to molecular dynamics results [20].

The Yukawa interaction can be written as

$$u(r) = \frac{a}{r}e^{-br}, \quad (17)$$

where a and b are parameters that can be fit to experimental data using the relation

$$S(k) = 1 + n\int d^3r[g(r) - 1]e^{-i\mathbf{k}\cdot\mathbf{r}}. \quad (18)$$

Then, given a mapping between a and b to basic quantities, which can be determined using some other method, these parameters serve as diagnostics. The total ionic energy may be known from an equation of state or other simulation method, which will constrain the thermodynamic dependencies of the parameters [21]. Once such a mapping has been accomplished, we can then exploit the known features of the reference system. The weakness of this approach is that it there may not be a unique mapping; for example, the total energy is an integral relation that permits a range of possible parameters. At a minimum, this methodology serves to define the effective coupling, through a, and the effective screening, through b, of the WDM as a Yukawa system. Then, many known properties of Yukawa systems, such as the equation of state [22], ionic diffusion [22], viscosity [8], and ionic thermal conductivity [22], can be approximately applied to the WDM.

C. Finite temperature Thomas-Fermi: separating bound from free states

In the present work, in particular in the steps around Eq. (15), the chemical picture is used, which allows the WDM structure problem to be broken into two steps. The first step involves finding a reasonable separation of bound and free states, and the second step involves assuming that the remaining steps (e.g., describing the screening) can employ linear approximations. In this subsection, the former step is discussed in detail.

Because WDM occurs at temperatures near or above the ionization energy, and because the density is high enough that pressure ionization contributes, the construction of a chemical picture model must include finite-temperature atomic physics at finite density. The simplest model for WDM is the cell model in which a nucleus is placed at the center of a spherical cell with a radius determined by the average volume occupied by that ion; typically, this is taken to be the ion-sphere radius a_i. The electronic structure is then computed inside the cell using an appropriate electronic structure theory. What is important is that all electrons (bound and free) are treated self-consistently in their interactions, their temperature, and their density. Here, the electronic structure is obtained using the finite-temperature Thomas-Fermi (FTTF) model. The Thomas-Fermi model, although not the most accurate model, tends to yield very accurate results at higher temperature, as considered here, at

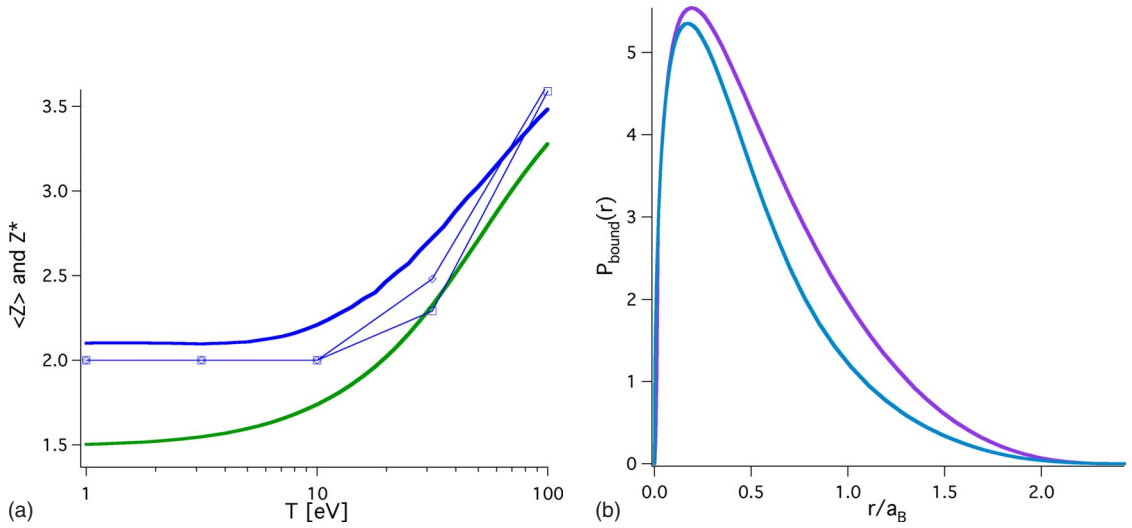

FIG. 4. (Color online) The predicted ionization state of Be is shown versus temperature for $\rho=1.69$ g/cm^3 (liquid density) using the two definitions of ionization discussed in the text. The upper (blue) curve corresponds to the definition Z^*, whereas the lower (green) curve corresponds to $\langle Z\rangle$. Also in the left panel, the thin blue lines with squares correspond to results obtained from a fully quantum mechanical calculation using the Z^* definition of the ionization state. The upper(diamonds)/lower(squares) thin blue curves neglect/include exchange correlation contributions, so that the relative effects of orbitals and exchange correlation can be disentangled. Note that there is good agreement between the fully quantal results and the TF model over a wide range of temperatures, indicating the reasonable efficacy of TF models for describing WDM. The right panel shows $P_{bound}(r)=4\pi r^2 n_{bound}(r)$ (arb. units) for Be at temperatures $T=1$ eV (upper, purple) and $T=20$ eV (lower, cyan), which shows how the bound density varies with increasing temperature and, therefore, ionization state.

higher density, and/or for heavier elements [23,24].

The FTTF begins with the Poisson equation

$$-\frac{1}{4\pi}\nabla^2 U(r) = -2e\int \frac{d^3p}{(2\pi\hbar)^3}\left[1+\exp\left\{\beta\left[\frac{p^2}{2m}+U(r)-\mu\right]\right\}\right]^{-1}+Ze\,\delta(\mathbf{r}), \tag{19}$$

which is a Poisson equation for the electron potential energy $U(r)$; the chemical potential μ is obtained by enforcing charge neutrality in the cell. Note that this equation is a nonlinear equation in the potential energy $U(r)$, which is treated here numerically to all orders. The main approximation made in Eq. (19) is that the kinetic energy contribution is taken to be that of a uniform Fermi gas. Once a solution has been obtained, the bound and free states can be separated from the resulting electron density. Unfortunately, the ionization state of WDM is not a well defined quantity. Typically, the ionization state is defined via the relation

$$\frac{4\pi}{3}a_i^3 n_e(a_i) = \langle Z\rangle, \tag{20}$$

which assumes that the electrons at the edge of the ion-sphere cell are the free electrons. However, one can also define the free electrons to be those with positive energy, which leads to the alternate definition

$$Z^* = \frac{1}{\pi^2\hbar^3}\int d^3r \int_{\sqrt{-2mU(r)}}^{\infty} dp p^2 \times\left[1+\exp\left\{\beta\left[\frac{p^2}{2m}+U(r)-\mu\right]\right\}\right]^{-1}. \tag{21}$$

Because the potential can be taken to vanish at the edge of the cell $[U(a_i)=0]$, we have $Z^*>\langle Z\rangle$. In constructing a chemical picture model, it is not clear which prescription is the more valid one; therefore, we will employ both and interpret the results as an uncertainty in the model. A comparison for Be is given in Fig. 4 [25].

If a simple Yukawa-like model is used, rather than a more precise screening function (15), the FTTF screening length is needed, which is given by

$$\lambda_{\mathrm{TF}} = \left(\frac{8\pi e^2\beta I'_{1/2}(\beta\mu)}{\Lambda^3}\right)^{-1/2} \equiv k_{\mathrm{TF}}^{-1} \approx \left(\frac{4\pi e^2 n_e\beta}{\sqrt{1+\left(\frac{2}{3}\beta E_F\right)^2}}\right)^{-1/2}, \tag{22}$$

where $\Lambda=\sqrt{2\pi\hbar^2\beta/m}$ is the thermal deBroglie wavelength, $I_{1/2}(x)$ is a Fermi integral, and the prime denotes differentiation with respect to the argument. An interpolation form is given in the third line, which is written in terms of the Fermi energy $E_F=\hbar^2(3\pi^2 n_e)^{2/3}/2m$. With these forms we can write the Yukawa potential as

$$u_Y(r) = \frac{\bar{Z}^2 e^2}{r}e^{-r/\lambda_{\mathrm{TF}}}, \tag{23}$$

where $\bar{Z}$ is either $\langle Z\rangle$ or Z^*, and n_e is the corresponding free electron density.

This section is concluded with a brief discussion of the merits of using the TF model for WDM, as defined here, or for other regimes of WDM. As the most important limitation of TF is the lack of orbitals, points are added to Fig. 4 from an orbital-based approach [26], but otherwise using the same approximations and using the Z^* definition; this result is shown as a thin blue line with diamonds. Clearly, the TF model captures the bulk of the physics across a wide range of temperatures. The major limitation is seen to be that TF strips the He-like core at too low of a temperature. The next most important limitation of TF is the lack of an exchange-correlation potential, and the orbital-based approach with exchange correlation is also shown as a thin blue line with squares; it is seen that this contribution is small. As Be is expected to challenge TF, we can conclude that the errors shown here are likely an upper bound, with heavier elements and higher densities having improved agreement. (Lower densities and/or lighter elements can be expected to be less well described by TF.) It remains to be seen whether gradient ("Weiszacker") corrections and exchange-correlation ("Dirac") corrections to such orbital-free density functional theories greatly extend its range of validity across a wide regime of WDM, although this may be the case [23,27]. Most importantly, these results show that the larger issue is the definition of the ionization—$\langle Z \rangle$ versus Z^*—not the method used to compute it [24].

D. Comparison with experimental data

It is necessary to justify the Yukawa model further, because of its various approximations. In general this is difficult to do because of the lack of theoretical and experimental results in the WDM regime. One can, however, compare predictions of this model to the very closely related system of liquid metals, which provides a fairly stringent test; such comparisons have been useful in other contexts [8]. Consider liquid Al (l-Al) just above the melting point. In this case, the ionization level is known to be $\bar{Z}=3$ (the FTTF model is not used here) and the free (valence) electrons are fully degenerate, so we can use the $\beta \to \infty$ limiting form of Eq. (22); the l-Al Yukawa model is completely specified. The liquid density is $\rho=2.27$ g/cm^3, which corresponds to ion and electron number densities of $n=5.03\times10^{22}$ cm^{-3} and $n_e=1.51\times10^{23}$ cm^{-3}, respectively. In this regime, the screening parameter is fixed at about $\kappa=3.37$, whereas the coupling parameter depends on the ion temperature. Figure 5 compares the structure factor from such a Yukawa model with experimental data [28]. Although the agreement is not perfect, the Yukawa model captures most of the features extremely well. What is not known is how such a result changes at the higher temperatures of WDM, although one would expect that the Yukawa model becomes even more accurate at high enough temperature.

E. Analytic structure factors and the Kirkwood line

Analytic structure factors are useful for obtaining rapid estimates that do not require sophisticated coding, and they provide some insight into the structure in those cases where the correct answer is known. When constructing analytic structure factors, it is useful to separate the problem into two pieces. For strongly coupled Coulomb systems, the asymptotic decay of the radial distribution function $g(r)$ is monotonic for small couplings and is damped oscillatory for larger couplings; these regimes can loosely be thought of as gaslike and liquidlike "phases" of the Coulomb system, although there is not a true critical point for purely repulsive Coulomb systems. The line in the phase diagram that separates the two behaviors is known as the Kirkwood line (KL). In practice, it is difficult to find an analytic structure factor that captures behavior on both sides of this line; and, in view of the WDM couplings shown in Fig. 3, it is necessary to find the location of the KL for WDM.

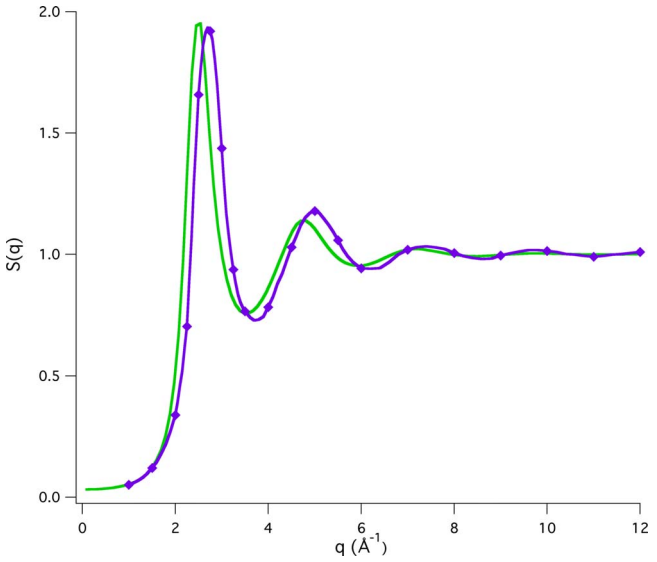

FIG. 5. (Color online) The Yukawa structure factor, using the HNCB method, for Al at just above the melting point ($\rho=2.27$ g/cm^{-3} and $T=0.114$ eV) is shown as a solid green line with no symbols. The purple curve with diamonds is the experimentally measured result.

Again, I take advantage of the fact that WDM is approximately a Yukawa system, for which the KL is known [29]. A fit to the numerical data yields

$$\Gamma_K(\kappa) = 1.21e^{\kappa/3.7}. \tag{24}$$

Interestingly, the KL does not parallel the melting line. In Fig. 6 the Coulomb couplings are shown versus temperature and density, just as they were in Fig. 3. Here, however, the value of the coupling is increased by 1/2 if the coupling is above Γ_K, and is decreased by 1/2 if the coupling is below Γ_K, in order to produce a discontinuity in the plot at $\Gamma_K(\kappa)$. In the WDM regime, as defined by the $\mathcal{W}$ parameter, Al is expected to have a much more liquidlike structure than Be, although both are largely liquidlike when $\mathcal{W}\sim1$.

Below the KL, the structure factor can be approximated by

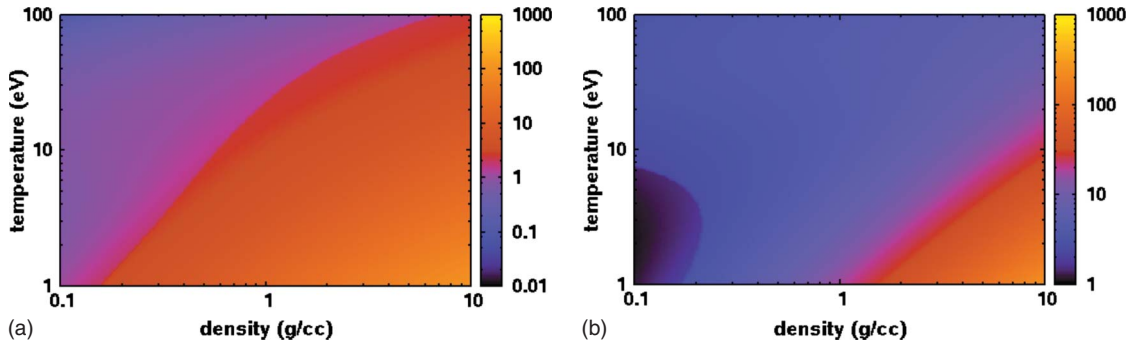

FIG. 6. (Color online) The Kirkwood lines for Be (left panel) and Al (right panel) are shown versus temperature and density. The figures show modified ion-ion Coulomb couplings with 1/2 added if the material is above the Kirkwood line and −1/2 added if it is below. Thus, the discontinuity in intensity/color is the boundary between monotonic and oscillatory decay of the pair correlation functions. Note that the location of the Kirkwood line is quite different for the different materials.

$$S(k) = \frac{k^2 + k_{\mathrm{TF}}^2[1 - G_{ee}(0)]}{k^2 + k_{\mathrm{TF}}^2[1 - G_{ee}(0)] + k_{Di}^2[1 - G_{ii}(k)]}, \tag{25}$$

which is derived in Appendix A. If the electrons are weakly coupled, $G_{ee}(0)$ can be neglected. An approximate $G_{ii}(k)$ is given by [30]

$$G_{ii}(k) = \frac{k^2}{k^2 + 4/a_i^2}, \tag{26}$$

where a_i is the ion-sphere radius; this form steepens $S(k)$ when k is of order the inverse interparticle spacing.

Above the KL, we use the fact that the structure factor is known analytically for the hard sphere system in the Percus-Yevick approximation. We begin by relating the structure factor to the direct correlation function (DCF) $c(r)$ as in Eq. (16); then, the DCF can be written as [31]

$$c(k) = -24\frac{\eta}{n}\int_0^1 ds s^2 \frac{\sin[qs(8\eta)^{1/3}]}{qs(8\eta)^{1/3}}[\alpha(\eta) + \beta(\eta)s + \gamma(\eta)s^2], \tag{27}$$

where

$$\alpha(\eta) = \frac{(1+2\eta)^2}{(1-\eta)^4}, \tag{28}$$

$$\beta(\eta) = -6\eta\frac{(1+\eta/2)^2}{(1-\eta)^4}, \tag{29}$$

$$\gamma(\eta) = \frac{\eta(1+2\eta)^2}{2(1-\eta)^4}. \tag{30}$$

The packing fraction η is given in terms of the HS diameter σ as $\eta = \pi n\sigma^3/6$.

Because of the focus here on Yukawa systems as a model for WDM, we can use the analytic structure factor if we can find a mapping between the HS system and the Yukawa system. This has been done using the Gibbs-Bogolyubov inequality [32], and the result, repeated here for completeness, is

$$\eta = a(\kappa) + \frac{b(\kappa)\ln(\Gamma)}{1 + c(\kappa)\ln(\Gamma)}, \tag{31}$$

$$a(\kappa) = 0.0255 - 0.0683\kappa + 0.0267\kappa^2 - 0.003\kappa^3, \tag{32}$$

$$b(\kappa) = 0.107\ \exp(-0.143\kappa - 0.105\kappa^2) \tag{33}$$

$$c(\kappa) = -0.116 + 0.134\ \exp(-0.19\kappa - 0.184\kappa^2). \tag{34}$$

Once the WDM parameters Γ and κ are obtained, using methods similar to those of the previous subsection, these formulas yield a simple, analytic form for the WDM structure factor, which may be used for rapid calculations of WDM structure. It is, however, useful to calibrate the accuracy of the form, since it relies on a mapping between HS and Yukawa systems and employs an approximation in the HS system. In Fig. 7, structure factors are shown for the full HNCB model, as compared with the analytical model. Although there is clearly some disagreement, the analytic model is within ~15% of the HNCB method. Two cases are shown, with the more strongly coupled case given by $\Gamma = 50$ and $\kappa = 1$, and the more weakly coupled case given by $\Gamma = 10$ and $\kappa = 1$. As the reason for the discrepancy may be that the Yukawa system is not well modeled by a HS system, the strongly screened case of $\Gamma = 50$ and $\kappa = 3$, which lies near the transition of HS behavior of the Yukawa system [33], is shown in Fig. 8, and the agreement is indeed improved. Moreover, recall that l-Al has $\kappa = 3.37$, which suggests that the analytical model presented here should be fairly accurate for strongly screened Yukawa systems, which in turn appear to accurately describe liquid metal data, as shown above. In comparison with a previous analytical model [34], the present model introduces the ionization level explicity through either Eqs. (20) or (21), and includes screening in a nonperturbative manner. Of course, when an HNCB calculation is available, that method should be used for comparison with experimental data.

V. DYNAMICS

Although current experiments are primarily focused on physics associated with the electrons and the diffraction due

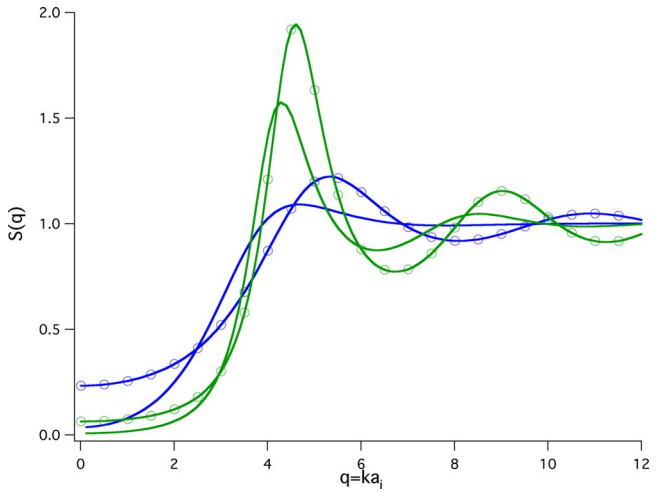

FIG. 7. (Color online) Comparison of the analytic structure factor with the hypernetted chain plus bridge result for two cases. The lower, more weakly coupled cases have $\Gamma=10$ and $\kappa=1$ (blue curves), whereas the upper, more strongly coupled cases have $\Gamma=50$ and $\kappa=1$ (green curves). The solid (no symbols) lines are HNCB results, and the lines with open circles are from the analytical model. In general, the analytical model tends to slightly overestimate the peak heights. This reveals the extent to which an effective coupling parameter model is useful.

to the ions, as discussed in detail above, the dynamics of the ions represents a greater theoretical challenge and could reveal information about collective modes, hydrodynamic behavior, and transport coefficients. In this section, models for the ion dynamics in WDM are considered, with the goals of giving predictions of wave dispersions, treating wave damping, possibly measuring the WDM viscosity, and to explore the limitations of hydrodynamics descriptions of WDM.

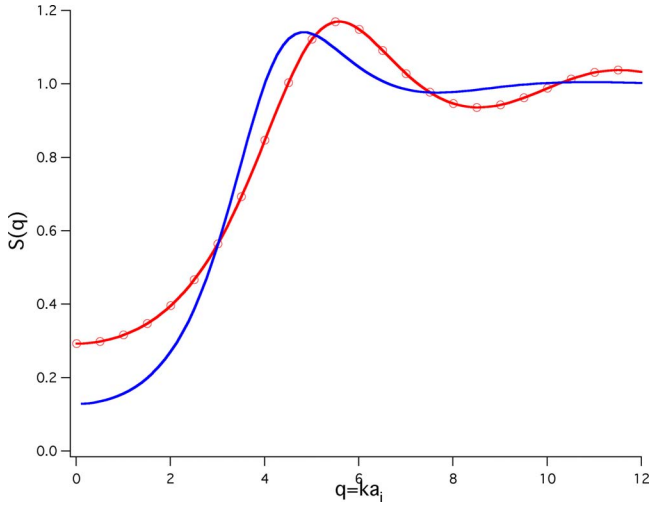

FIG. 8. (Color online) Comparison of the analytic structure factor with HNCB results (blue line with no symbols), as in the previous figure, but for the case $\Gamma=50$ and $\kappa=3$. In this case, the actual system is closer to a real HS system (red line with circles), and the resulting agreement is improved. Thus, for strongly screened WDM, most of the ionic structure can be accounted for by simple HS repulsion; the remainder is due to details of the electronic structure.

A. Plasmon pole models

In this subsection, so-called "plasmon-pole" models will be considered. In these models, the dynamics are assumed to peak over narrow enough frequency intervals that the ii-DSF is expressible in terms of delta functions. Thus, in general, the full spectrum is not obtainable, but ion acoustic wave (IAW) dispersion relations are. Two models will be discussed here that serve to reveal some important issues associated with IAWs in WDM.

The simplest model of the ii-DSF is given by

$$S^{(1)}(k,\omega) = \pi \mathcal{B}^{(1)}(k)\,\delta[\omega \pm \mathcal{C}^{(1)}(k)], \tag{35}$$

where the unknown coefficients $\mathcal{B}^{(1)}(k)$ and $\mathcal{C}^{(1)}(k)$ can be determined by enforcing exact sum rules. This expression should be compared with Eq. (6). Unfortunately, the result is not unique because there are infinitely many pairs of sum rules that can be used. If we use Eq. (7) with the f-sum rule

$$F(k) = \int_{-\infty}^{\infty} \frac{d\omega}{2\pi}\omega^2 S(k,\omega) = \frac{k^2}{\beta M}, \tag{36}$$

the dispersion relation of the IAW is

$$\mathcal{C}^{(1)}(k) = \sqrt{\frac{k^2}{\beta M S(k)}}, \tag{37}$$

which has been obtained previously [34]. This result reveals that the dynamics of the IAW are largely describable using any of the techniques described above for obtaining $S(k)$. For example, using Eq. (25) in the long-wavelength limit, the IAW dispersion relation is

$$\omega(k) = v_{th}k\sqrt{\frac{k_{\mathrm{TF}}^2[1-G_{ee}(0)] + k_{Di}^2[1-G_{ii}(0)]}{k_{\mathrm{TF}}^2[1-G_{ee}(0)]}}, \tag{38}$$

where the ion thermal velocity $v_{th}^2 = 1/\beta M$ has been defined. The IAW dispersion relation clearly contains a wealth of information about the state of the WDM. However, beyond the issue that an arbitrary choice of sum rules has been made to obtain this result, the form (35) itself is also not unique. Generalizing Eq. (35), we can include the possibility of a low-frequency diffusional mode, and write

$$S^{(2)}(k,\omega) = 2\pi \mathcal{A}^{(2)}(k)\,\delta(\omega) + \pi \mathcal{B}^{(2)}(k)\,\delta[\omega \pm \mathcal{C}^{(2)}(k)]. \tag{39}$$

This form includes three unknowns that can be determined by using the previous sum rules and

$$I(k) = \int \frac{d\omega}{2\pi}\omega^4 S(k,\omega) = \frac{3k^4}{\beta M} + \frac{k^2 n}{\beta M^2}\int d^3 r g(r)[1-\cos(kz)]\frac{\partial^2 u(r)}{\partial z^2}. \tag{40}$$

Note that, in writing Eq. (40), an effective pair potential $u(r)$ between ions, such as Eq. (23), is assumed. This model yields the relations

$$\mathcal{A}^{(2)}(k) = \frac{S(k)I(k) - F^2(k)}{I(k)},$$

$$\mathcal{B}^{(2)}(k) = \frac{F^2(k)}{I(k)},$$

$$\mathcal{C}^{(2)}(k) = \sqrt{\frac{I(k)}{F(k)}}. \tag{41}$$

Note that the higher-order sum rules modify the strength of the diffusive mode near $\omega \sim 0$ relative to the model given by Eq. (8). More importantly, the collective mode at frequency $\omega(k)=\mathcal{C}^{(2)}(k)$ has changed considerably relative to $\mathcal{C}^{(1)}(k)$ in Eq. (37).

It is worth noting that the result (41) differs from the result obtained by Gregori *et al.* [34]. The discrepancy can be traced to their use of a form similar to Eq. (35), which neglects the diffusive mode [$\mathcal{A}(k)=0$]. By neglecting this contribution, their model is subject to the particular choice of sum rules used, since only two sum rules are required; that is, they employed Eqs. (7) and (36), whereas they could have equally well used Eqs. (36) and (40). In the model presented here, three sum rules are employed simultaneously, and we find that the collective mode is determined predominantly by Eq. (40) rather than by Eq. (7). In fact, the result obtained here is essentially a generalization of the so-called quasilocalized charge approximation [35], as applied to WDM, which works very well for strongly coupled Coulomb systems. This point raises the important issue that, in fact, there are infinitely many sum rules that are not used here. In principle, if we employed higher-order sum rules, we could also include damping of the modes by broadening the delta functions in Eq. (39). Unfortunately, the remaining sum rules depend on quantities more complicated [36] than the radial distribution function $g(r)$, and are difficult to use in practice. Another limitation of the plasmon-pole method is that it does not yield the full spectrum. For this reason, the most common approach to computing DSFs is to employ the fluctuation-dissipation theorem (FDT) to relate the DSF to the relevant response function(s). In the FDT approach, one begins with the random phase approximation (RPA) and adds dynamic local field corrections to include non-RPA physics such as collisions [37]. Here, we take the different approach of using generalized hydrodynamics (GH), which begins with a very different starting point.

B. Generalized hydrodynamics approaches: Wave damping

In the GH approach, one begins with the hydrodynamic equations as a starting point and adds corrections that incorporate important constraints; the GH method has the advantage that the beyond-RPA contributions of viscous damping and of the exact compressibility appear even in the simplest description. Recently, the GH approach has been applied to XRTS in WDM [8]. Here, we extend that work to interpret the plasmon pole models and to include corrections that satisfy an additional sum rule.

To illustrate the GH method, we begin with the (linearized) Navier-Stokes (NS) equation for the ion current, which reads

$$nM\frac{\partial \mathbf{j}(\mathbf{r},t)}{\partial t} = -\nabla P(\mathbf{r},t) + \eta\nabla^2\mathbf{j}(\mathbf{r},t) + (\eta/3+\zeta)\,\nabla\nabla\cdot\mathbf{j}(\mathbf{r},t), \tag{42}$$

where M is the ion mass, η is the shear viscosity, ζ is the bulk viscosity, and P is the pressure. From the longitudinal part of this we can find the NS ii-DSF, which takes the form

$$S_{NS}(k,\omega) = \frac{2v_{th}^2k^4\nu_l}{\left(\omega^2 - \dfrac{k^2}{nM\chi_T}\right)^2 + (\omega\nu_l k^2)^2}. \tag{43}$$

Details of the GH method, showing the connection between Eqs. (42) and (43), are given in Appendix B. Note that, formally, the "exact" compressibility χ_T and longitudinal kinematic viscosity $\nu_l=(\frac{4}{3}\eta+\zeta)/(nM)$ already appear at this level. If we have methods to compute these quantities, and we restrict ourselves to the hydrodynamic regime (long wavelengths and low frequencies), Eq. (43) would give a good description of WDM ion dynamics that includes strong coupling through both χ_T and ν_l, and collisional damping through ν_l. Conversely, this form could be fit to experimental data to extract χ_T and ν_l.

The dispersion of IAW in the NS approximation is

$$\omega_{NS}(k) = \sqrt{\frac{k^2}{nM\chi_T} - \frac{\nu_l^2k^4}{2}}, \tag{44}$$

which includes a shift in the location of the resonance to wave damping. Away from the resonance, at very high frequency, the NS equation predicts asymptotic decay of ω^{-4}, suggesting that the sum rule (7) can be applied. This yields a modifed NS (MNS) ii-DSF of the form

$$S_{MNS}(k,\omega) = \frac{2v_{th}^2k^4\nu_l}{\left(\omega^2 - \dfrac{k^2}{\beta MS(k)}\right)^2 + (\omega\nu_l k^2)^2} \tag{45}$$

$$\omega_{MNS}(k) = \sqrt{\frac{k^2}{\beta MS(k)} - \frac{\nu_l^2k^4}{2}}. \tag{46}$$

The k dependence is now changed at shorter wavelengths, away from the hydrodynamic limit. Note that this result is consistent with $\lim_{k\to 0} S(k)=nT\chi_T$, where $\chi_T=n^{-1}\partial n/\partial P$. Interestingly, Eq. (45) implies that higher-order spatial derivatives *should* appear in Eq. (42); thus, Eq. (45) generalizes Eq. (42) to shorter length scales. Moreover, Eq. (46) describes IAWs with the same basic dispersion as Eq. (37), but with a collisional shift, which would otherwise have been been very difficult to obtain using the plasmon-pole method. The result (46) shows that Eq. (37) corresponds to the hydrodynamic limit, as generalized to all length scales. That is, both Eqs. (37) and (46) are low-frequency results, in contrast to Eq. (41) which is a high-frequency result. Because of the asymptotic decay of $S_{MNS}(k,\omega)$, higher-order sum rules are divergent and, therefore, inconsistent with Eq. (41). The ul-

timate source of this discrepancy is that the NS equation only contains a single time derivative. Because WDM is predicted to have an IAW, the dispersion of the wave could potentially probe both low, as described by Eq. (37), and high, as described by Eq. (41), frequency regimes; this behavior is not generally shared by the electrons, which tend to only probe high-frequency (elasticlike) physics. Building upon the MNS equation, we may extend Eq. (45) by considering more complicated memory functions [36]. For example, the form [38]

$$S_3(k,\omega) = \frac{2\tau F(k)\{[\mathcal{C}^{(2)}(k)]^2 - F^2(k)/S(k)\}}{[\omega^2 - F(k)/S(k)]^2 + \{\omega\tau[\omega^2 - \mathcal{C}^{(2)}(k)\}^2} \quad (47)$$

satisfies all of the three sum rules considered so far, independent of effective collision time τ. Matching to the MNS form at $\omega=0$ relates τ to the viscosity, and we obtain

$$S_3(k,\omega) = \frac{2v_{th}^2 k^4 \nu_l}{[\omega^2 - F(k)/S(k)]^2 + \left\{\omega\nu_l k^2 \dfrac{\omega^2 - [\mathcal{C}^{(2)}(k)]^2}{F(k)/S(k) - [\mathcal{C}^{(2)}(k)]^2}\right\}^2}, \quad (48)$$

which now explicitly contains viscous damping, asymptotically decays as ω^{-6}, and contains information from the three basic sum rules. The damping of IAWs has recently been obtained using a sum rule approach [39] that uses a highly approximate form for the damping rate. In contrast, the GH method employed here circumvents this difficulty by relating the damping to a well known quantity, the viscosity, that can be computed very accurately using molecular dynamics. Moreover, the present GH method suggests a method for an experimental measurement of an important transport property of WDM.

C. Dark resonance

It is clear that the asymptotic frequency behavior of the ii-DSF is a very important factor in determining the validity regime of a given theoretical model, and is something that could potentially be measured experimentally. However, there is an important modification to the high-frequency behavior in the XRTS signal that occurs because the x-rays scatter by the electrons, and not the ions. To see this, consider WDM for which the Compton contribution to Eq. (5) is unimportant, such as fully ionized WDM. Then, the FDT relates the ee-DSF to the full electron-electron response function

$$\chi_{ee}(k,\omega) = \Delta^{-1}(k,\omega)\{\chi_e^{(0)}(k,\omega) \times\{1 - u_{ii}(k)\chi_i^{(0)}(k,\omega)[1 - G_{ii}(k,\omega)]\}\}$$

$$\Delta(k,\omega) = \{1 - u_{ee}(k)\chi_e^{(0)}(k,\omega)[1 - G_{ee}(k,\omega)]\} \times\{1 - u_{ii}(k)\chi_i^{(0)}(k,\omega)[1 - G_{ii}(k,\omega)]\} - u_{ei}^2(k)\chi_i^{(0)} \times(k,\omega)\chi_e^{(0)}(k,\omega)[1 - G_{ei}(k,\omega)]^2. \quad (49)$$

This form is the dynamical generalization of Eq. (A6). In obtaining the Chihara result (5), one adds and subtracts the electron jellium contribution

$$\chi_{ee}^{jell}(k,\omega) = \chi_e^{(0)}(k,\omega)/\{1 - u_{ee}\chi_e^{(0)}(k,\omega)[1 - G_{ee}(k,\omega)]\} \quad (50)$$

to obtain

$$\chi_{ee}(k,\omega) = \chi_{ee}^{jell}(k,\omega) + \left\{\frac{\chi_e^{(0)}(k,\omega)u_{ei}(k)[1 - G_{ei}(k,\omega)]}{1 - u_{ee}\chi_e^{(0)}(k,\omega)[1 - G_{ee}(k,\omega)]}\right\}^2 \times\frac{\chi_i^{(0)}(k,\omega)\{1 - u_{ee}(k)\chi_e^{(0)}(k,\omega)[1 - G_{ee}(k,\omega)]\}}{\Delta(k,\omega)}. \quad (51)$$

The first term in Eq. (51) corresponds to the first term in Eq. (5), whereas the second term here corresponds to the final term in Eq. (5), provided that the factor in large square brackets is taken to be real and frequency independent (static), which is reasonable since it multiplies the term $\chi_i^{(0)}(k,\omega)$. The low-frequency spectrum would thus be determined by $S(k,\omega)$. However, such a result neglects the fact that, in the original expression (49), the numerator contains an ion contribution that, when

$$1 - u_{ii}(k)\chi_i^{(0)}(k,\omega)[1 - G_{ii}(k,\omega)] = 0, \quad (52)$$

causes the *numerator* to vanish. Note that this is just the condition for an ion plasma wave, which will always occur just above the IAW. Thus, because the radiation scatters from the electrons, the measured asymptotic form of the low-frequency spectrum has such a modification. This is a "dark resonance" because it produces a minimum, rather than a maximum, at the resonance condition [40]. Note that the dark resonance is missing from the Chihara formulation (5) because of the way in which the jellium dynamics is separated from terms that are treated at zero frequency. Such a dark resonance could be used as a diagnostic, if it could be seen, because of the specific form of the resonance determined by Eq. (52).

VI. SUMMARY AND OUTLOOK

In summary, the low-frequency portion of the WDM XRTS signal has been considered. WDM has been defined

here in terms of the parameter $\mathcal{W}$, which is useful for establishing regimes of matter for which the coupling and degeneracies are both of order unity. This definition was chosen because it highlights the regime for which both theory and experiment are particularly difficult. At normal density, WDM tends to occur at temperatures near 10 eV, with $\mathcal{W}$ largest at slightly lower temperatures and densities. A key quantity in WDM is the ionization state, which strongly affects the correlations at a given temperature and density. The importance of finite-temperature, finite-density atomic physics has been emphasized in this context. Here, a simple Thomas-Fermi model has been used that yields all-electron density information (bound and free), including the ionization state, in an all-electron, self-consistent formulation. However, it has been shown that the ionization state is ambiguous in the WDM regime, and two definitions of the ionization state have been discussed. Although corrections to Thomas-Fermi (e.g., gradient corrections, exchange-correlation potential) could also be included, the most important improvement is likely to be in the inclusion of the structure factor directly in the electronic structure calculation [27,41].

The QOZE were then used to reduce the WDM problem to an effective dressed-particle system amenable to classical methods. Importantly, the sequence of approximations that leads to such a description was noted, and further research is warranted to understand the magnitude of error made in each step. For example, it is currently not known if one can treat the electron-ion interaction weakly, as is done with liquid metals, because the conditions that lead to a weak interaction may not be met in WDM. A discussion of the QOZE is given in Appendix A, and several useful results are derived. Having a dressed-particle model for WDM then led to a discussion of the diffraction (frequency integrated) signal.

Here, based on the dressed-particle picture, a Yukawa model was proposed, with the caveats just mentioned, that has implicitly finite-temperature atomic physics, via the FTTF model used to separate bound and free states, and a finite-temperature and density screening length. Thus, despite its potential inaccuracy, the Yukawa model applies across wide ranges of material conditions. More importantly, many useful results can be immediately obtained from previous studies of Yukawa systems, such as bridge functions, viscosities, etc. The accuracy of this approach was validated by comparison with liquid metal data, which represents an extreme limit of the WDM regime, and very good agreement was found. If the assumptions leading to the Yukawa model are valid away from this regime, one expects that the Yukawa model very accurately describes WDM. Here, the parameters of the Yukawa model arise from the FTTF result and an expression for the screening length. However, one can also treat the Yukawa parameters as fitting parameters that can be fit to, for example, the energy in a quantum molecular dynamics calculation; then, the effective Yukawa model so obtained can be used to obtain all other dynamical quantities from a classical molecular dynamics simulation.

The full dynamical spectrum $S(k,\omega)$ for the ions was then addressed. Plasmon-pole approximations were discussions and some ambiguities were revealed in the use of sum rules to constrain the parameters. As there are only three sum rules that are nontrivial (i.e., they do not involve correlation functions beyond the two-particle level), the best possible plasmon-pole approximation is one that includes a zero frequency diffusion mode and IAW peaks. This leads to a dispersion relation that differs from that of previous work, and is similar to that obtained using the quasilocalized approximation that has been shown to be quite accurate for strongly coupled systems in general. According to the definition given here for WDM, however, WDM is only moderately coupled, a situation that is potentially more interesting because diffusion and damping can play a larger role. Thus, it is important to develop models that go beyond the simple sum rule approach, and, here, a GH approach has been employed. GH models have the distinct advantage that the full spectrum is given even in their simplest form; details are given in Appendix B. Moreover, the main inputs are the compressibility and viscosity, which include strong coupling and damping, thereby placing a different emphasis on requirements for the theory. The sum rules have also been shown to be useful, and their use reveals the validity regime of the basic hydrodynamics equations, which do not in general satisfy the sum rules. Thus, the GH models allow us to explore the physics of WDM hydrodynamics and its breakdown at finite length and time scales. In the hydrodynamic limit, viscous damping of the IAW mode may allow the WDM viscosity to be measured. An important issue for the future is quantum corrections [42] to the classical $S(k,\omega)$, which will modify the frequency spectrum at higher frequencies.

Many of the ideas presented here may impact future experiments on facilities that have recently been constructed. For example, the National Ignition Facility (NIF) [43] is now operating, with the goal of achieving ignition by 2012. This facility can easily probe the entire WDM regime, including the higher temperature regimes considered in the present work; a comprehensive experimental study that includes measurements that span the cold solid to hot plasma regimes will provide constraints on theoretical models, such as equations of state, that attempt to span that difficult regime. The key to success, of course, is that detailed measurements of temperatures and densities can be made of the matter under study. Here, I have detailed the various approximations that enter into various models (e.g., number of sum rules used, weak coupling approximations, damping, etc.) that are used to infer physical properties from low-frequency XRTS data. By focusing on low frequencies, I have shown that the viscosity of a strongly coupled plasma can be measured; the viscosity plays an important role in the hydrodynamic evolution of implosions, but has never been measured under relevant conditions. Moreover, I have shown that a dark resonance is possible, which suggests a method for measuring the ionic plasmon mode directly in NIF targets. Such an additional spectral feature provides further, independent diagnostic information.

ACKNOWLEDGMENT

The author wishes to thank Stephanie Hansen (Sandia National Laboratories) for providing orbital-based results on the ionization of Be.

APPENDIX A: QUANTUM ORNSTEIN ZERNIKE EQUATIONS

Most treatments of WDM structure begin with the classical structure equations and effective quantum potentials. As it is not clear that such an approach is appropriate for WDM [3], the quantum mechanical forms for the structure equations are reviewed in this appendix. The analysis centers on the quantum mechanical Orstein-Zernike equations (QOZE), which are shown to yield powerful results that do not rely on effective potentials.

Classical strongly coupled mixtures of species i and j can be described by the set of structure equations

$$h_{ij}(k) = c_{ij}(k) + \sum_l n_l c_{il}(k) h_{lj}(k), \tag{A1}$$

$$g_{ij}(r) = \exp[-\beta u_{ij}(r) + h_{ij}(r) - c_{ij}(r) + B_{ij}(r)], \tag{A2}$$

where $h_{ij}(r) = g_{ij}(r) - 1$ are the pair correlation functions in terms of the radial distribution functions $g_{ij}(r)$, $c_{ij}(r)$ are the direct correlation functions, the $B_{ij}(r)$ are the bridge functions, and the n_l are the average species densities. The structure factors are obtained via

$$S_{ij}(k) = 1 + \sqrt{n_i n_j} \int d^3 r [g_{ij}(r) - 1] e^{-i\mathbf{k}\cdot\mathbf{r}} \tag{A3}$$

$$= 1 + \sqrt{n_i n_j} h_{ij}(k). \tag{A4}$$

As these equations are classical, they are not directly applicable to warm dense matter (WDM). Often, the pair interactions $u_{ij}(r)$ are modified to incorporate quantum corrections, although recent research [3] suggests that such an approach is quite limited for WDM due to issues with atomic physics and partial degeneracy. However, for classical systems, the structure factors are related to the density-density response functions through

$$S_{ij}(k) = -\frac{T}{\sqrt{n_i n_j}} \chi_{ij}(k), \tag{A5}$$

which suggests an alternate route.

The quantum mechanical response functions for a two-component plasma are given formally as [44]

$$\chi_{11}(k) = D^{-1}(k) \chi_1^{(0)}(k) \{1 - v_{22}(k) \chi_2^{(0)}(k) [1 - G_{22}(k)]\},$$

$$\chi_{12}(k) = D^{-1}(k) v_{12}(k) \chi_1^{(0)}(k) \chi_2^{(0)}(k) [1 - G_{12}(k)],$$

$$\chi_{22}(k) = D^{-1}(k) \chi_2^{(0)}(k) \{1 - v_{11}(k) \chi_1^{(0)}(k) [1 - G_{11}(k)]\},$$

$$\begin{aligned} D(k) = {} & \{1 - v_{11}(k) \chi_1^{(0)}(k) [1 - G_{11}(k)]\} \\ & \times \{1 - v_{22}(k) \chi_2^{(0)}(k) [1 - G_{22}(k)]\} - v_{12}^2(k) \chi_1^{(0)}(k) \chi_2^{(0)}(k) \\ & \times [1 - G_{12}(k)][1 - G_{21}(k)]. \end{aligned} \tag{A6}$$

The local field corrections $G_{ij}(k)$ are introduced, which can be considered to be the terms that make this formulation *exact*; the random phase approximation is recovered when $G_{ij}(k) = 0$. These response functions are polarizabilities that are defined according to the convention

$$\delta n_i(k) = \sum_j \chi_{ij}(k) U_j(k), \tag{A7}$$

where $U_j(k)$ is an interaction energy that couples only to species j. The Eqs. (A6) are the QOZE, and they generalize Eq. (A2) to WDM. In this form, the QOZE are equations for the $\chi_{ij}(k)$ in terms of the known quantities $\chi_i^{(0)}(k)$ and $v_{ij}(k)$, and the unknown $G_{ij}(k)$. Additional information is needed to close the QOZE.

The QOZE can be used to derive many powerful relations very easily. For example, the ratio of the second and first equations gives (exactly)

$$\frac{\chi_{12}(k)}{\chi_{11}(k)} = \frac{v_{12}(k) \chi_2^{(0)}(k) [1 - G_{12}(k)]}{\{1 - v_{22}(k) \chi_2^{(0)}(k) [1 - G_{22}(k)]\}}. \tag{A8}$$

This result relates the correlations between species 1 and 2 to the correlations within species 1; this ratio is referred to as the pseudoatom density (PD). As a second example, the first equation in Eq. (A6) can be taken to be the structure factor of the ions. If the electron-ion interaction is weak, the interactions are mostly Coulomb-like, and the electron screening can be taken in the long-wavelength (Thomas-Fermi) limit, then the ion-ion structure factor

$$S_{ii}(k) = \frac{k^2 + k_{TF}^2 [1 - G_{ee}(0)]}{k^2 + k_{\mathrm{TF}}^2 [1 - G_{ee}(0)] + k_{Di}^2 [1 - G_{ii}(k)]} \tag{A9}$$

is obtained. Here, k_{Di} and k_{TF} are the state-dependent Debye and Thomas-Fermi wave vectors, respectively, and the electron-electron local field correction $G_{ee}(k)$ is taken in the long-wavelength limit to be consistent with the treatment of $\chi_e^{(0)}(k)$. Obviously, the power of the more general result (A6) is that the approximations leading to Eq. (A9) can be relaxed.

A closer connection between the formulation given in the main text and the approach given here can be made by making the identification [45]

$$c_{ij}(k) = -\beta v_{ij}(k) [1 - G_{ij}(k)], \tag{A10}$$

which relates the direct correlation functions to the local field corrections. Together with Eq. (A5), Eq. (A10) changes variables in the QOZE from $\chi_{ij}(k)$ and $G_{ij}(k)$ to $\chi_{ij}(k)$ and $S_{ij}(k)$, depending on the quantal nature of the species, and $c_{ij}(k)$. Again, the system is not yet closed until a relation between the functions is given. If species 1 are the (classical) nuclei and species 2 are the (quantal) electrons, then (A8) can be written in the more common form

$$\frac{S_{eN}(k)}{S_{NN}(k)} = -\beta^{-1} c_{eN}(k) \sqrt{\frac{n_N}{n_e}} \tilde{\chi}_{ee}(k) \tag{A11}$$

$$\equiv n_{pa}(k), \tag{A12}$$

where the last step defines the PD. As in the main text, it is assumed that $\tilde{\chi}_{ee}(k)$ is taken to be approximately the jellium response for an electron gas of arbitrary temperature and density. Results such as these provide exact starting points for obtaining approximate models of WDM, as has been carried out in the main text. Moreover, in the context of XRTS, the particular result (A11) is useful since it more directly

relates the physics of the ion-ion structure to the observable quantity, since x-rays are predominantly scattered by the electrons.

The pseudoatom density corresponding to the model used in the main text can be readily obtained by replacing nuclear variables with ionic variables (chemical picture), and therefore assuming a weak electron-ion interaction. For this case, the relevant "Yukawa PD" relations are

$$-\beta^{-1}c_{ei}(k) \approx \frac{4\pi\langle Z\rangle e^2}{k^2}, \tag{A13}$$

$$\chi_e^{(0)}(k) \approx -\frac{k_{\mathrm{TF}}^2}{4\pi e^2}, \tag{A14}$$

$$n_{pa}^{(Y)}(k) = -\frac{\sqrt{\langle Z\rangle}k_{\mathrm{TF}}^2}{k^2 + k_{\mathrm{TF}}^2[1 - G_{ee}(0)]}. \tag{A15}$$

The first approximation corresponds to a weak $e-i$ interaction, whereas the second approximation is to employ long-wavelength forms; together, one obtains a PD of Yukawa form that is applicable to arbitrary temperature and density WDM. Here, the screening length is determined by k_{TF}, the state-dependent Thomas-Fermi screening wave vector, as modified by non-RPA corrections contained in $G_{ee}(0)$. Shorter wavelength corrections can also be added [46], but will not be considered here.

APPENDIX B: GENERALIZED HYDRODYNAMICS

Some basic ideas from generalized hydrodynamics (GH) are presented here with the aim of providing insight into the GH method and to provide a derivation of Eq. (43). The GH method begins with the microscopic density and current variables

$$n(\mathbf{r},t) = \frac{1}{\sqrt{N}}\sum_{i=1}^{N}\delta[\mathbf{r} - \mathbf{r}_i(t)],$$

$$\mathbf{j}(\mathbf{r},t) = \frac{1}{\sqrt{N}}\sum_{i=1}^{N}\mathbf{v}_i\delta[\mathbf{r} - \mathbf{r}_i(t)], \tag{B1}$$

where $\mathbf{r}_i(t)$ and $\mathbf{v}_i(t)$ are the phase space variables for each particle i. Note that these variables satisfy a microscopic continuity equation of the form

$$\frac{\partial n(\mathbf{r},t)}{\partial t} = -\nabla\cdot\mathbf{j}(\mathbf{r},t). \tag{B2}$$

These equations are referred to as "microscopic" because no averaging or initial conditions have been included. Typically, an ensemble-averaged phase space function $f(\mathbf{r},\mathbf{v})$ is formed, the quantities in Eq. (B1) are constructed from obvious integrals over $f(\mathbf{r},\mathbf{v})$, and an appropriate kinetic equation is derived to describe the many-body dynamics. The challenge with this approach is that collisions are very difficult to include for strongly coupled systems. The goal of the GH method is to include collisions in an exact manner within an approximate, but reasonable framework.

In the GH method, we assume in analogy with Eq. (B2) that we can also obtain a microscopic equation for $\partial\mathbf{j}(\mathbf{r},t)/\partial t$. One way to obtain such an equation is to note that the equations of motion for a fluid in the low frequency and long-wavelength limit are well established [47]; such equations of motion are referred to as hydrodynamics equations. The most widely used hydrodynamics equation is the Navier-Stokes (NS) equation, which includes viscous (collisional) damping. It is therefore reasonable to assume that the microscopic Eqs. (B1) also satisfy the NS in the appropriate limit. If so, and this can be tested, then collisions are included via the viscosity, which can be determined nearly exactly from the Kubo-Green relation using molecular dynamics, once the effective ion-ion interactions have been determined. Thus, we assume the relation [this is just Eq. (42) repeated here for convenience]

$$nM\frac{\partial\mathbf{j}(\mathbf{r},t)}{\partial t} = -\nabla P(\mathbf{r},t) + \eta\nabla^2\mathbf{j}(\mathbf{r},t) + (\eta/3+\zeta)\nabla\nabla\cdot\mathbf{j}(\mathbf{r},t) \tag{B3}$$

for the microscopic current in Eq. (B1). If we have an equation of state $P(\mathbf{r},t)$ that depends only on the density fluctuations, then Eqs. (B2) and (B3) form a closed set of equations.

It is worth pausing to discuss the strengths and weaknesses of what has been presented so far. First, the entire approach is somewhat phenomenological in that one supposes that the *microscopic* variables satisfy the NS equation. Second, the NS is by no means exact, and caution is in order with applying results away from the hydrodynamic limit; this is addressed in detail in the main text, and is the reason that *generalized* hydrodynamics is necessary. Third, the strengths are that the equation of state and viscous collisions appear in their exact form in the basic equations of motion. Note that the closure here is through the equation of state, which is assumed not to introduce fluctuations beyond those being considered. It remains to be determined what level of closure is actually appropriate for WDM, and thermal conduction (an additional energy equation that includes temperature fluctuations) should be explored in the future.

Let us now Fourier transform the NS in space and select the longitudinal portion. Doing so yields the equation

$$nM\frac{\partial j_l(k,t)}{\partial t} = -ikP(k,t) - \eta_l k^2 j_l(k,t), \tag{B4}$$

where the longitudinal viscosity is given by $\eta_l = \frac{4}{3}\eta + \zeta$. Because this is a microscopic equation, we can multiply through by the initial condition $j_l(-k,0)$ and perform an ensemble average $\langle\cdots\rangle$, which then reads

$$nM\frac{\partial J_l(k,t)}{\partial t} = -ik\langle P(k,t)j_l(-k,0)\rangle - \eta_l k^2 J_l(k,t), \tag{B5}$$

where $J_l(k,t) = \langle j_l(k,t)j_l(-k,0)\rangle$ is the current-current correlation function. A specific form for the equation of state needs to be specified to proceed. Very importantly for Coulomb systems is that the pressure term must include a contribution $-\nabla U(\mathbf{r},t)$ from long-range interactions; here, that is to be

determined from the effective ion-ion interaction. Typically, the $P(\mathbf{r},t)$ and $-\nabla U(\mathbf{r},t)$ terms introduce density dependencies, which can be eliminated with the continuity equation. The resulting equation can be solved for $J_l(k,\omega)$ and related to the dynamic structure factor via the exact relationship $S(k,\omega)=k^2J_l(k,\omega)/\omega^2$.

In the vast majority of calculations of the DSF, the fluctuation dissipation theorem (FDT) is used to relate the imaginary part of a response function to the dynamic structure factor. That approach can also be used here by including a weak external potential in the NS equation that drives density fluctuations. The result is the same. Within the GH method, however, we see how to obtain the DSF directly without the intermediate steps associated with the FDT, since we obtain an equation of motion for the correlation function itself, as in Eq. (B5).

[1] R. W. Lee *et al.*, J. Opt. Soc. Am. B **20**, 770 (2003); S. H. Glenzer and R. Redmer, Rev. Mod. Phys. **81**, 1625 (2009).
[2] A. Ng, T. Ao, F. Perrot, M. W. C. Dharma-Wardana, and M. E. Foord, Laser Part. Beams **23**, 527 (2005).
[3] C. S. Jones and M. S. Murillo, High Energy Density Phys. **3**, 379 (2007).
[4] H. M. Van Horn, Science **252**, 384 (1991).
[5] B. H. Ripin *et al.*, Laser Part. Beams **8**, 183 (1990); E. G. Gamaly, *ibid.* **12**, 185 (1994).
[6] J. F. Benage, W. R. Shanahan, and M. S. Murillo, Phys. Rev. Lett. **83**, 2953 (1999).
[7] M. H. Key, Phys. Plasmas **14**, 055502 (2007).
[8] M. S. Murillo, High Energy Density Phys. **4**, 49 (2008).
[9] M. W. C. Dharma-wardana and M. S. Murillo, Phys. Rev. E **77**, 026401 (2008); M. S. Murillo and M. W. C. Dharma-wardana, Phys. Rev. Lett. **100**, 205005 (2008).
[10] N. Nettelmann, B. Holst, A. Kietzmann, M. French, R. Redmer, and D. Blaschke, Astrophys. J. **683**, 1217 (2008).
[11] R. Ernstofer, M. Harb, C. T. Hebelson, G. Sciani, T. Dartgalongue, R. J. D. Miller, Science **323**, 1033 (2009).
[12] S. H. Glenzer *et al.*, Phys. Rev. Lett. **98**, 065002 (2007).
[13] Z. Donkó, G. J. Kalman, and K. I. Golden, Phys. Rev. Lett. **88**, 225001 (2002); J. Hubbard and J. L. Beeby, J. Phys. C **2**, 556 (1969).
[14] R. M. More, K. H. Warren, D. A. Young, and G. B. Zimmerman, Phys. Fluids **31**, 3059 (1988).
[15] J. Chihara, J. Phys.: Condens. Matter **12**, 231 (2000).
[16] S. Sahoo, G. F. Gribakin, G. Shabbir Naz, J. Kohanoff, and D. Riley, Phys. Rev. E **77**, 046402 (2008).
[17] G. Gregori, S. H. Glenzer, W. Rozmus, R. W. Lee, and O. L. Landen, Phys. Rev. E **67**, 026412 (2003).
[18] J. Chihara, Prog. Theor. Phys. **59**, 76 (1978).
[19] A. A. Louis and N. W. Ashcroft, Phys. Rev. Lett. **81**, 4456 (1998); J. Non-Cryst. Solids **250-252**, 9 (1999).
[20] W. Daughton, M. S. Murillo, and L. Thode, Phys. Rev. E **61**, 2129 (2000).
[21] D. Alfé, G. Kresse, and M. J. Gillan, Phys. Rev. B **61**, 132 (2000).
[22] Z. Donkó, J. Phys. A **42**, 214029 (2009).
[23] P. Fromy, C. Deutsch, and G. Maynard, Phys. Plasmas **3**, 714 (1996).
[24] M. S. Murillo *et al.*, High Energy Density Phys. (to be published).
[25] F. Perrot, Phys. Rev. E **47**, 570 (1993).
[26] S. B. Hansen *et al.*, Phys. Rev. E **72**, 036408 (2005).
[27] E. Smargiassi and P. A. Madden, Phys. Rev. B **49**, 5220 (1994).
[28] http://www.tagen.tohoku.ac.jp
[29] P. Hopkins, A. J. Archer, and R. Evans, Phys. Rev. E **71**, 027401 (2005).
[30] M. S. Murillo, Phys. Plasmas **5**, 3116 (1998).
[31] N. W. Ashcroft and J. Lekner, Phys. Rev. **145**, 83 (1966).
[32] M. S. Murillo, Phys. Rev. E **62**, 4115 (2000).
[33] G. Faussurier and M. S. Murillo, Phys. Rev. E **67**, 046404 (2003).
[34] G. Gregori, A. Ravasio, A. Höll, S. H. Glenzer, and S. J. Rose, High Energy Density Phys. **3**, 99 (2007).
[35] K. I. Golden and G. J. Kalman, Phys. Plasmas **7**, 14 (2000).
[36] J. P. Boon and S. Yip, *Molecular Hydrodynamics* (Dover, New York, 1980).
[37] M. S. Murillo, Phys. Plasmas **7**, 33 (2000).
[38] S. W. Lovesey, J. Phys. C **4**, 3057 (1971).
[39] G. Gregori and D. O. Gericke, Phys. Plasmas **16**, 056306 (2009).
[40] J. Daligault and M. S. Murillo, Phys. Rev. E **68**, 015401(R) (2003).
[41] D. Ofer, E. Nardi, and Y. Rosenfeld, Phys. Rev. A **38**, 5801 (1988).
[42] M. D. Srinivas, M. S. Sriram, and T. S. Shankara, Int. J. Theor. Phys. **5**, 263 (1972).
[43] E. I. Moses, Nucl. Fusion **49**, 104022 (2009).
[44] S. Ichimaru, S. Mitake, S. Tanaka, and X.-Z. Yan, Phys. Rev. A **32**, 1768 (1985).
[45] J. A. Anta and A. A. Louis, Phys. Rev. B **61**, 11400 (2000).
[46] K. Nagao, S. A. Bonev, and N. W. Ashcroft, Phys. Rev. B **64**, 224111 (2001).
[47] Landau and Lifshitz, *Fluid Mechanics* (Butterworth and Heinemann, Oxford, 1997).